

# The `pde2path` add-on toolbox `p2poc` for solving infinite time–horizon spatially distributed optimal control problems

– Quickstart Guide –

Hannes Uecker<sup>1</sup>

<sup>1</sup> Institut für Mathematik, Universität Oldenburg, D26111 Oldenburg, hannes.uecker@uni-oldenburg.de

July 8, 2015

## Abstract

`p2poc` is an add-on toolbox to the `Matlab` continuation and bifurcation package `pde2path`. It is aimed at the numerical analysis of infinite time horizon optimal control (OC) problems for parabolic systems of PDE over 1D or 2D spatial domains. The basic idea is a two step approach to the canonical systems, derived from Pontryagin’s Maximum Principle. First we use `pde2path` to find branches of stationary solutions of the canonical system, also called canonical steady states (CSS). In a second step we use the results and the spatial discretization of the first step to calculate the objective values of time-dependent canonical paths connecting to a CSS with the so called saddle point property. This is a (high dimensional) boundary value problem (BVP) in time, which we solve by combining a modification of the BVP solver TOM with a continuation algorithm in the initial states. We explain the design and usage of the package via two example problems, namely the optimal management of a distributed shallow lake, and of a semi-arid grazing system. Both show interesting bifurcations of so called patterned CSS, and in particular the latter also a variety of patterned *optimal* steady states. The package (library and demos) can be downloaded at [www.staff.uni-oldenburg.de/hannes.uecker/pde2path](http://www.staff.uni-oldenburg.de/hannes.uecker/pde2path).

## 1 Introduction

Denoting the state variable (vector) by  $v = v(t, x) \in \mathbb{R}^N$ , and the control by  $k = k(t, x) \in \mathbb{R}$ , we consider spatially distributed infinite time horizon optimal control (OC) problems of the form

$$V(v_0(\cdot)) := \max_{k(\cdot, \cdot)} J(v_0(\cdot), k(\cdot, \cdot)), \quad J(v_0(\cdot), k(\cdot, \cdot)) := \int_0^\infty e^{-\rho t} J_{ca}(v(t), k(t)) dt, \quad (1a)$$

$$\text{where } J_{ca}(v(\cdot, t), k(\cdot, t)) = \frac{1}{|\Omega|} \int_\Omega J_c(v(x, t), k(x, t)) dx \quad (1b)$$

is the spatially averaged current value objective function, with the local current value  $J_c: \mathbb{R}^{N+1} \rightarrow \mathbb{R}$  a given function;  $\rho > 0$  is the discount rate, and  $v: \Omega \times [0, \infty) \rightarrow \mathbb{R}^N$  fulfills a PDE of the form

$$\partial_t v = -G_1(v, k) := D\Delta v + g_1(v, k), \quad v|_{t=0} = v_0. \quad (1c)$$

Here,  $D \in \mathbb{R}^{N \times N}$  is a diffusion matrix,  $\Delta = \partial_{x_1}^2 + \dots + \partial_{x_d}^2$  is the Laplacian, and (1c) holds in a bounded domain  $\Omega \subset \mathbb{R}^d$  with suitable boundary conditions (BC), where for simplicity we restrict to homogeneous Neumann  $\partial_\nu v = 0$ ,  $\nu$  the outer normal. In applications,  $J_c$  and  $G_1$  of course often also depend on a number of parameters, which however for simplicity we do not display here.<sup>1</sup> The discounted time integral in (1a) is typical for economic problems, where “profits now” weight more than mid or far future profits. More specifically,  $\rho$  corresponds to a long-term investment

---

<sup>1</sup> $G_1$  in (1c) can in fact be of a much more general form, but for simplicity here we stick to (1c). The convention that  $\partial_t v = -G_1(v)$  instead of  $\partial_t v = G_1(v)$  with  $G_1(v) = D\Delta v + g_1(v)$  is inherited via `pde2path` from the `Matlab` `pde toolbox`, which assembles  $-\Delta$  into the stiffness matrix  $K$ .

rate. We have  $J_{ca}$  normalized by  $|\Omega|$  for easier comparison between different domains and space dimensions. Finally, the max in (1a) runs over all *admissible* controls  $k$ ; this essentially means that  $k \in L^\infty([0, \infty) \times \Omega, \mathbb{R})$ , and we do not (yet) consider explicit control or state constraints. For general references and comments on OC for PDE problems, see Remark 1.1 below.

Introducing the costates  $\lambda : \Omega \times (0, \infty) \rightarrow \mathbb{R}^N$  and the (local current value) Hamiltonian

$$\mathcal{H} = \mathcal{H}(v, \lambda, k) = J_c(v, k) + \lambda^T (D\Delta v + g_1(v, k)), \quad (2)$$

by Pontryagin's Maximum Principle (see Remark 1.1) for  $\tilde{\mathcal{H}} = \int_0^\infty e^{-\rho t} \overline{\mathcal{H}}(t) dt$  with the spatial integral

$$\overline{\mathcal{H}}(t) = \int_{\Omega} \mathcal{H}(v(x, t), \lambda(x, t), k(x, t)) dx, \quad (3)$$

an optimal solution  $(v, \lambda)$  (or equivalently  $(v, k) : \Omega \times [0, \infty) \rightarrow \mathbb{R}^{N+1}$ ) has to solve the canonical system (CS)

$$\partial_t v = \partial_\lambda \mathcal{H} = D\Delta v + g_1(v, k), \quad v|_{t=0} = v_0, \quad (4a)$$

$$\partial_t \lambda = \rho \lambda - \partial_v \mathcal{H} = \rho \lambda + g_2(v, k) - D\Delta \lambda, \quad (4b)$$

where  $k = \operatorname{argmax}_{\tilde{k}} \mathcal{H}(v, \lambda, \tilde{k})$ , which generally we assume to be obtained from solving

$$\partial_k \mathcal{H}(v, \lambda, k) = 0. \quad (4c)$$

Under suitable concavity conditions on  $J_c$  this holds due to the absence of control constraints. The costates  $\lambda$  also fulfill zero flux BC, and derivatives like  $\partial_v \mathcal{H}$  etc are taken variationally, i.e., for  $\overline{\mathcal{H}}$ . For instance, for  $N = 1$  and  $\Phi(v, \lambda) := \lambda \Delta v$  we have  $\overline{\Phi}(v, \lambda) = \int_{\Omega} \lambda \Delta v dx = \int_{\Omega} (\Delta \lambda) v dx$  by Gauß' theorem, hence  $\delta_v \overline{\Phi}(v, \lambda)[h] = \int (\Delta \lambda) h dx$ , and by the Riesz representation theorem we identify  $\delta_v \overline{\Phi}(v, \lambda)$  and hence  $\partial_v \Phi(v, \lambda)$  with the multiplier  $\Delta \lambda$ .

In principle we want to solve (4) for  $t \in [0, \infty)$ , but in (4a) we have initial data for only half the variables, and in (4b) we have anti-diffusion, such that (4) is ill-posed as an initial value problem. For convenience we set

$$u(t, \cdot) := \begin{pmatrix} v(t, \cdot) \\ \lambda(t, \cdot) \end{pmatrix} : \Omega \rightarrow \mathbb{R}^{2N}, \quad (5)$$

and write (4) as

$$\partial_t u = -G(u, \eta) := \mathcal{D}\Delta u + f(u), \quad \text{where } \mathcal{D} = \begin{pmatrix} D & 0 \\ 0 & -D \end{pmatrix}, \quad f(u) = \begin{pmatrix} g_1(u) \\ g_2(u) \end{pmatrix}, \quad (6a)$$

and where  $\eta \in \mathbb{R}^p$  stands for parameters present, which for instance also includes the discount rate  $\rho$ . Besides the boundary condition  $\partial_\nu u = 0$  and the initial condition

$$v|_{t=0} = v_0, \quad (6b)$$

we then impose the transversality condition

$$\lim_{t \rightarrow \infty} e^{-\rho t} u(t) = 0. \quad (6c)$$

A solution  $u$  of the canonical system (6) is called a *canonical path*, and an equilibrium of (6a) (which automatically fulfils (6c)) is called a *canonical steady state (CSS)*. With a slight abuse of notation we also call  $(v, k)$  with  $k$  given by (4d) a canonical path. See also, e.g., [GU15] for more formal definitions, further comments on the notions of optimal systems, and, e.g., the significance of the transversality condition (6c).

**Remark 1.1.** For general background on OC in a PDE setting see [Trö10] and the references therein, or specifically [RZ99a, RZ99b] and [AAC11, Chapter5] for Pontryagin’s Maximum Principle for OC problems for semilinear diffusive models. However, these works are in a finite time horizon setting, and often the objective function is linear in the control and there are control constraints, e.g.,  $k(x, t) \in K$  with some bounded interval  $K$ . Therefore  $k$  is not obtained from the analogue of (4c), but rather takes the values from  $\partial K$ , which is often called bang–bang control. In, e.g., [CPB12, ACKLT13], some specific models have been studied in this setting and a rather theoretical way, i.e., the focus is on deriving the canonical system and showing well-posedness and the existence of an optimal control. [ADS14] additionally contains numerical simulations for a finite time horizon control–constrained OC problem for a three species spatial predator-prey system, again leading to bang–bang type controls. See also [NPS11] and the references therein for numerical methods for (finite time horizon) constrained parabolic optimal control problems. Here we do not (yet) consider (active) control or state constraints, and no terminal time, but the infinite time horizon. ]

Using the canonical system (4) we proceed in two steps, which can be seen as a variant of the “connecting orbit method”, see, e.g., [BPS01] and [Gra15, Chapter 7]: first we compute (branches of) CSS, and second we compute canonical paths connecting to some CSS. This also means that we take a somewhat broader perspective than aiming at computing just one optimal control, given an initial condition  $v_0$ , which without further information is ill-posed anyway. Instead, our method aims to give a somewhat global picture by identifying the optimal CSS and their respective domains of attraction.

**(a) CSS branches.** We compute (approximate) CSS of (6), i.e., solutions  $\hat{u}$  of

$$G(u, \eta) = 0, \tag{7}$$

together with the BC. For this we use the package `pde2path` [UWR14, DRUW14] to set up a FEM discretization of (7) as a continuation/bifurcation problem in one of the parameters, which we call  $\eta$  again. This gives branches  $\eta \mapsto \hat{u}(\eta)$  of solutions, which is in particular useful to possibly find several solutions  $\hat{u}^{(l)}(\eta)$ ,  $j = l, \dots, m$  at fixed  $\eta$ . By computing the associated  $J_{ca}(\hat{v}^{(l)}, k^{(l)})$  we can identify which of these is optimal amongst the CSS. Given a CSS  $\hat{u}$ , for simplicity we also write  $J_{ca}(\hat{u}) := J_{ca}(\hat{v}^{(l)}, k^{(l)})$ , and moreover, have

$$J(\hat{u}) = J_{ca}(\hat{u})/\rho. \tag{8}$$

**(b) Canonical paths.** In a second step (b), using the spatial discretization and the results from (a), we calculate canonical paths connecting to a CSS  $\hat{u}$  (and often starting at the state values  $\hat{v}_0$  of a different CSS  $\hat{u}_0$ ), and the objective values of the canonical paths. For this we choose a truncation time  $T$  and modify (6c) to the condition that  $u(T) \in W_s(\hat{u})$  and near  $\hat{u}$ , where  $W_s(\hat{u})$  denotes the stable manifold of  $\hat{u}$ . In practice, we approximate  $W_s(\hat{u})$  by the stable eigenspace  $E_s(\hat{u})$ , and thus consider the BVP

$$\partial_t u = -G(u), \tag{9a}$$

$$v|_{t=0} = v_0, \tag{9b}$$

$$u(T) \in E_s(\hat{u}) \text{ (and } \|u(T) - \hat{u}\| \text{ small)}. \tag{9c}$$

If the mesh in the FEM consists of  $n$  nodes, then  $u(t) \in \mathbb{R}^{2Nn}$ , and (9a) yields a system of  $2Nn$  ODEs in the form (with a slight abuse of notation)

$$M \frac{d}{dt} u = -G(u), \tag{10a}$$

while the initial and transversality conditions become

$$v|_{t=0} = v_0, \quad (10b)$$

$$\Psi(u(T) - \hat{u}) = 0 \text{ (and } \|u(T) - \hat{u}\| \text{ small)}. \quad (10c)$$

Here  $M \in \mathbb{R}^{2Nn \times 2Nn}$  is the mass matrix of the FEM mesh, and  $\Psi \in \mathbb{R}^{Nn \times 2Nn}$  defines the projection onto  $E_u(\hat{u})$ . Moreover, (10b) consists of  $Nn$  initial conditions for the states, while the costates  $\lambda$  (and hence the control  $k$ ) are free. Thus, to have  $2Nn$  BC altogether we need  $\dim E_s(\hat{u}) = Nn$ . On the other hand, we always have  $\dim E_s(\hat{u}) \leq Nn$ , see [GU15, Appendix A]. We define the defect

$$d(\hat{u}) := \dim E_s(\hat{u}) - Nn \quad (11)$$

and call a CSS  $\hat{u}$  with  $d(\hat{u}) = 0$  a CSS with the saddle–point property (SPP). At first sight it may appear that  $d(\hat{u})$  depends on the spatial discretization, i.e., on the number of  $n$  of nodes. However,  $d(\hat{u})$  remains constant for finer and finer meshes, see [GU15, Appendix A] for further comments.

For  $\hat{u} = (\hat{v}, \hat{\lambda})$  with the SPP, and  $\|v_0 - \hat{v}\|$  sufficiently small, we may expect the existence of a solution  $u$  of (10), which moreover can be found from a Newton loop for (10) with initial guess  $u(t) \equiv \hat{u}$ . On the other hand, for larger  $\|v_0 - \hat{v}\|$  a solution of (10) may not exist, or a good initial guess may be hard to find, and therefore we use a continuation process also for (10). In the simplest setting, assume that for some  $\alpha \in [0, 1]$  we have a solution  $u_\alpha$  of (10) with (10b) replaced by

$$v(0) = \alpha v_0 + (1 - \alpha)\hat{v}, \quad (12)$$

(e.g.,  $\alpha = 0$  and  $u \equiv \hat{u}$ ). We then increase  $\alpha$  by some stepsize  $\delta_\alpha$  and use  $u_\alpha$  as initial guess for (10a), (10c) and (12), ultimately aiming at  $\alpha = 1$ .

To actually solve (10a), (10c) and (12) we use TOM [MS02, MT04, MST09] in a version `mtom` which accounts for the mass matrix  $M$  on the lhs of (10a).<sup>2</sup> This predictor ( $u_\alpha$ ) – corrector (`mtom` for  $\alpha + \delta_\alpha$ ) continuation method corresponds to a “natural” parametrization by  $\alpha$ , and is thus implemented in `p2poc` as `iscnat` (Initial State Continuation NATural). We also give the option to use a secant predictor

$$u^j(t) = u^{j-1}(t) + \delta_\alpha \tau(t), \quad \tau(t) = (u^{(j-1)}(t) - u^{(j-2)}(t)) / \|u^{(j-1)}(\cdot) - u^{(j-2)}(\cdot)\|_2, \quad (13)$$

where  $u^{j-2}$  and  $u^{j-1}$  are the two previous steps. However, the corrector still works at fixed  $\alpha$ , in contrast to the arclength predictor–corrector `iscarc` described next.

It may happen that no solution of (10a), (10c) and (12) is found for  $\alpha > \alpha_0$  for some  $\alpha_0 < 1$ , i.e., that the continuation to the intended initial states fails. In that case, often the BVP shows a fold in  $\alpha$ , and we use a modified continuation process, letting  $\alpha$  be a free parameter and using a pseudo–arclength parametrization by  $\sigma$  in the BC at  $t = 0$ . Since `mtom` does not allow free parameters we add the dummy ODE  $\dot{\alpha} = 0$ , and BCs at continuation step  $j$ ,

$$\left\langle s, (u(0) - u^{(j-1)}(0)) \right\rangle + s_\alpha (\alpha - \alpha^{(j-1)}) = \sigma, \quad (14)$$

with  $(u^{(j-1)}(\cdot), \alpha^{j-1})$  the solution from the previous step, and  $(s, s_\alpha) \in \mathbb{R}^{2Nn} \times \mathbb{R}$  appropriately chosen with  $\|(s, s_\alpha)\|_* = 1$ , where  $\|\cdot\|_*$  is a suitable norm in  $\mathbb{R}^{2Nn+1}$ , which may contain different weights of  $v$  and  $v_\alpha$ . For  $s = 0$  and  $s_\alpha = 1$  we find `iscnat` with stepsize  $\delta_\alpha = \sigma$  again. To get around folds we may use the secant

$$s := \xi (u^{(j-1)}(0) - u^{(j-2)}(0)) / \|u^{(j-1)}(0) - u^{(j-2)}(0)\|_2 \text{ and } s_\alpha = 1 - \xi$$

---

<sup>2</sup>`mtom` is an ad-hoc modification of TOM, and will be replaced by an official version of TOM which handles mass matrices once that becomes available. In the following, when discussing, e.g., the behaviour and usage of `mtom`, we note that almost all of this is derived from TOM. See also [www.dm.uniba.it/~mazzia/mazzia/?page\\_id=433](http://www.dm.uniba.it/~mazzia/mazzia/?page_id=433)

with small  $\xi$ , and also a secant predictor

$$(u^j, \alpha^j)^{\text{pred}} = (u^{j-1}, \alpha^{j-1}) + \sigma\tau \quad (15)$$

for  $t \mapsto u^j(t)$  with

$$\tau = \xi(u^{(j-1)}(\cdot) - u^{(j-2)}(\cdot)) / \|u^{(j-1)}(\cdot) - u^{(j-2)}(\cdot)\|_2 \text{ and } \tau_\alpha = 1 - \xi. \quad (16)$$

This essentially follows [GCF<sup>+</sup>08, §7.2], and is implemented in a routine `iscarc` (Initial State Continuation ARClength).

Finally, given  $\hat{u}$ , to calculate  $\Psi$ , at startup we solve the generalized adjoint eigenvalue problem

$$\partial_u G(\hat{u})^T \Phi = \Lambda M \Phi \quad (17)$$

for the eigenvalues  $\Lambda$  and (adjoint) eigenvectors  $\Phi$ , which also gives the defect  $d(\hat{u})$  by counting the negative eigenvalues in  $\Lambda$ . If  $d(\hat{u}) = 0$ , then from  $\Phi \in \mathbb{C}^{2Nn \times 2Nn}$  we generate a real base of  $E_u(\hat{u})$  which we sort into the matrix  $\Psi \in \mathbb{R}^{Nn \times 2Nn}$ .

**Acknowledgement.** I thank D. Grass, ORCOS Wien, for introducing me to the field of optimal control over infinite time horizons, and for clarifying (and posing) many questions regarding the aim of software based on Pontryagin's Maximum Principle for spatially distributed OC problems.

## 2 Examples and implementation details

We now explain how to use `p2poc` to calculate CSS and canonical paths for two example problems of type (1), namely the SLOC (Shallow Lake Optimal Control) and the vegOC (vegetation Optimal Control) problems. For this we discuss `Matlab` files from the demo directories `slocdemo` and `vegdemo`, assuming that `slocdemo` and `vegdemo` are in the same directory as the libraries `p2plib`, `p2poclib` and `tom`, see [www.staff.uni-oldenburg.de/hannes.uecker/pde2path](http://www.staff.uni-oldenburg.de/hannes.uecker/pde2path) for all downloads.

The current version of `pde2path` is based on the `Matlab` `pdetoolbox`, and thus works most efficiently for spatial 2D problems, while 1D problems are treated as narrow quasi 1D strips. This is not elegant, and inefficient, but the latter hardly matters for the core functionality of `pde2path`, i.e., the computation of stationary bifurcation diagrams. However, efficiency is an issue for canonical paths, and thus it is useful to replace the `pdetoolbox` by genuine 1D routines. Here we use the package `OOPDE`, which is a free, object oriented, `Matlab` FEM package for 1D, 2D and 3D problems that in some interfaces mimicks the behaviour of the `pdetoolbox`, see [www.mathe.tu-freiberg.de/nmo/mitarbeiter/uwe-pruefert/software](http://www.mathe.tu-freiberg.de/nmo/mitarbeiter/uwe-pruefert/software). However, as `OOPDE` is currently under heavy development, and as so far we only use a small fraction of the capabilities of `OOPDE` in `p2poc`, here we first explain the use of `p2poc` based on the old `pdetoolbox`, and refer to §3 for the genuine 1D setup based on `OOPDE`.

### 2.1 The SLOC model

Following [BX08], in [GU15] we consider a model for phosphorus  $P = P(t, x)$  in a shallow lake, and phosphate load  $k = k(x, t)$  as a control, which in 0D, i.e., in the ODE setting, has been analyzed in detail for instance in [KW10]. Here we explain how we set up the spatial so called Shallow Lake Optimal Control (SLOC) problem in `p2poc`, and refer to [GU15] for details about the modelling and the interpretation of results. The model reads

$$V(P_0(\cdot)) := \max_{k(\cdot, \cdot)} J(P_0(\cdot), k(\cdot, \cdot)), \quad J(P_0(\cdot), k(\cdot, \cdot)) := \int_0^\infty e^{-\rho t} J_{ca}(P(t), k(t)), dt \quad (18a)$$

where  $J_c(P, k) = \ln k - \gamma P^2$ ,  $J_{ca}(P(t), k(t)) = \frac{1}{|\Omega|} \int_{\Omega} J_c(P(x, t), k(x, t)) dx$  as in (1b), and  $P$  fulfills the PDE

$$\partial_t P(x, t) = k(x, t) - bP(x, t) + \frac{P(x, t)^2}{1 + P(x, t)^2} + D\Delta P(x, t), \quad (18b)$$

$$\partial_\nu P(x, t)_{\partial\Omega} = 0, \quad P(x, t)_{t=0} = P_0(x), \quad x \in \Omega \subset \mathbb{R}^d. \quad (18c)$$

The parameter  $b > 0$  is the phosphorus degradation rate, and  $\gamma > 0$  are ecological costs of the phosphorus contamination  $P$ . One wants a low  $P$  for ecological reasons, but for economical reasons a high phosphate load  $k$ , for instance from fertilizers used by farmers. Thus, the objective function consists of the concave increasing function  $\ln k$ , and the concave decreasing function  $-\gamma P^2$ . In `slocdemo` we consider two scenarios, namely

$$\text{Scenario 1: } D = 0.5, \rho = 0.03, \gamma = 0.5, b \in (0.5, 0.8) \text{ (primary bif. param.)}, \quad (19)$$

$$\text{Scenario 2: } D = 0.5, \rho = 0.3, b = 0.55, \gamma \in (2.5, 3.7) \text{ (primary bif. param.)}, \quad (20)$$

but here we restrict to Scenario 1, and refer to [Gra15] for discussion of the results of Scenario 2.

With the co-state  $q$  and local current value Hamiltonian

$$\mathcal{H}(P, q, \lambda) = J_c(P, k) + q \left[ k - bP + \frac{P^2}{1 + P^2} + D\Delta P \right], \quad (21)$$

the canonical system for (18) becomes, with  $k(x, t) = -\frac{1}{q(x, t)}$ ,

$$\partial_t P(x, t) = k(x, t) - bP(x, t) + \frac{P(x, t)^2}{1 + P(x, t)^2} + D\Delta P(x, t), \quad (22a)$$

$$\partial_t q(x, t) = 2\gamma P(x, t) + q(x, t) \left( \rho + b - \frac{2P(x, t)}{(1 + P(x, t)^2)^2} \right) - D\Delta q(x, t), \quad (22b)$$

$$\partial_\nu P(x, t)_{\partial\Omega} = 0, \quad \partial_\nu q(x, t)_{\partial\Omega} = 0, \quad P(x, t)_{t=0} = P_0(x), \quad x \in \Omega. \quad (22c)$$

### 2.1.1 Basics of `pde2path`, and the setup for CSS

We very briefly review the data structures of `pde2path`, and refer to [UWR14, DRUW14] for more details and the underlying algorithms. The basic structure is a `Matlab` struct, henceforth called `p` like problem, which has a (large) number of fields (and subfields), as indicated in Table 1. However,

Table 1: Selection (with focus on the semilinear case `p.sw.sfem=1`) of fields in the structure `p` describing a `pde2path` problem; see `stanparam.m` in `p2plib` for detailed information on the contents of these fields and the standard settings.

field	purpose
<code>fuha</code>	struct of <b>function handles</b> ; in particular the function handles <code>p.fuha.sG</code> , <code>p.fuha.sGjac</code> , <code>p.fuha.bc</code> , <code>p.fuha.bcjac</code> defining (6a) and Jacobians.
<code>nc, sw</code>	<b>numerical controls and switches</b> such as <code>p.sw.bifcheck</code> , ...
<code>u, np, nu</code>	the solution <code>u</code> (including all parameters/auxiliary variables in <code>u(p.nu+1:end)</code> ), the number of nodes <code>p.np</code> in the mesh, and the number of nodal values <code>p.nu</code> of PDE-variables
<code>tau, branch</code>	tangent <code>tau(1:p.nu+p.nc.nq+1)</code> , and the branch, filled via <code>bradat.m</code> and <code>p.fuha.outfu</code> .
<code>sol</code>	other values/fields calculated at runtime, e.g.: <code>ds</code> (stepsize), <code>res</code> (residual), ...
<code>usrlam</code>	vector of user set target values for the primary parameter, default <code>usrlam=[]</code> ;
<code>eqn, mesh</code>	the tensors <code>c, a, b</code> for the semilinear FEM setup, and the geometry data and mesh.
<code>plot, file</code>	switches (and, e.g., figure numbers and directory name) for plotting and file output
<code>mat</code>	problem matrices, e.g., mass/stiffness matrices $M, K$ for the the semilinear FEM setting.

most of these can be set to standard values by calling `p=stanparam(p)`. In standard problems the user only has to provide:

1. The geometry of the domain  $\Omega$  and the boundary conditions.
2. Function handles (in the semilinear setting of interest here) `sG` implementing  $G$ , and, for speedup, `sGjac`, implementing the Jacobian.
3. An initial guess for a solution  $u$  of  $G(u) = 0$ , i.e., an initial guess for a CSS.

Table 2: The init routine `slinit.m`, the rhs `slsG.m`, the objective function `sljcf.m`, and the function `slcon.m`. See also, e.g., the source code of `slsGjac` for the implementation of  $G_u$ .

```

1 function p=slinit(p,lx,ly,nx,ny,sw) % init-routine
2 p=stanparam(p); % set generic parameters to standard, if needed reset below..
3 p.nc.neq=2; p.fuha.sG=@slsG; p.fuha.sGjac=@slsGjac; %rhs
4 p.fuha.outfu=@ocbra; p.fuha.jcf=@sljcf; p.fuha.con=@slcon; % current-val-obj
5 p.usrlam=[0.55 0.6 0.65 0.7 0.75]; % target-values for bif-param lam
6 [p.mesh.geo,bc]=recnbc2(lx,ly); p.vol=4*lx*ly; % geometry, and volume of dom
7 p.fuha.bc=@(p,u) bc; p.fuha.bcjac=@(p,u) bc; % standard Neumann BC
8 p.xplot=lx; p.sw.spcalc=0; p.sw.jac=1; p.file.smod=100; % some more switches
9 par=[0.03;0.55;0.5;0.5]; p.nc.ilam=2; % startup param values, and index of main param
10 % r=par(1); bp=par(2); cp=par(3); D=par(4);
11 p.nc.dsmin=1e-6; p.nc.dsmax=0.5; p.nc.lammax=0.8; p.nc.lammin=0.549; p.sol.ds=0.1;
12 p=stanmesh(p,nx,ny);p=setbmesh(p); p.sol.xi=1/p.np; % mesh
13 p.eqn.c=[1;0;0;1;-1;0;0;-1]; p.eqn.a=0; p.eqn.b=0; % diffusion tensor and a,b
14 switch sw % choose initial guess arcoording to switch
15 case 1; u=0.3*ones(p.np,1); v=-13*ones(p.np,1); u0=[u v]; p.u=u0(:); % FSC
16 case 2; u=2*ones(p.np,1); v=-4*ones(p.np,1); u0=[u v]; p.u=u0(:); % FSM
17 case 3; .. % Scenario 2
18 end
19 p.u=[p.u; par]; p.sw.sfem=1; p=setfemops(p); % semilin. setting
20 [p.u,res]=nloop(p,p.u); fprintf('first res=%g\n',res); plotsol(p,1,1,1);

1 function r=slsG(p,u) % CS for SLOC, p_t=D*lap p-1/q-b*p+p^2/(1+p^2)
2 % q_t=-D lap q+2cp*p+q*(rho+bp-2*p/(1+p^2))^2;
3 par=u(p.nu+1:end); r=par(1); bp=par(2); cp=par(3); D=par(4);
4 P=u(1:p.np); q=u(p.np+1:2*p.np);
5 f1=-1./q-bp*P+P.^2./(1+P.^2); f2=2*cp*P+q.*(r+bp-2*P./(1+P.^2).^2);
6 f=[f1;f2]; r=D*p.mat.K*u(1:p.nu)-p.mat.M*f;

1 function jc=sljcf(p,u) % current value J
2 cp=u(p.nu+3:end); pv=u(1:p.np); kv=-1./u(p.np+1:p.nu); jc=log(kv)-cp*pv.^2;

1 function k=slcon(p,u) % extract control from states/costates
2 k=-1./u(p.np+1:p.nu);

```

Typically, the steps 1-3 are put into an init routine, here `p=slinit(p,lx,ly,nx,ny,sw,rho)`, where `lx,ly,nx,ny` are parameters to describe the domain size and discretization, and `sw` is used to set up different initial guesses, see Table 2. For CSS computations the only additions/modifications to the standard `pde2path` setting are as follows: (the additional function handle) `p.fuha.jc` should be set to the local current value objective function, here `p.fuha.jc=@sljcf`, and `p.fuha.outfu` to `ocbra`, i.e., `p.fuha.outfu=@ocbra`. This automatically puts  $J_{ca}(u)$  at position 4 of the calculated output-branch. Finally, it is useful to set `p.fuha.con=@slcon`, where `k=slcon(p,u)` extracts the control  $k$  from the states  $v$ , costates  $\lambda$  and parameters  $\eta$ , all contained in the vector  $u$ .<sup>3</sup>

By calling `p=cont(p)`, `pde2path` then first uses a Newton-loop to converge to a (numerical) CSS, and afterwards attempts to continue in the given parameter. If `p.sw.bifcheck>0`, then `pde2path` detects, localizes and saves to disk bifurcation points on the branch. Afterwards, the

<sup>3</sup>We do not use `slcon` in `slsG`. However, putting this function into `p` has the advantage that for instance plotting and extracting the value of the control can easily be done by calling some convenience functions of `p2poc`.

bifurcating branches can be computed by calling `swibra` and `cont` again. These (and other) `pde2path` commands (continuation, branch switching, and plotting) are typically put into a script file, here `bdcmds.m`, see Table 3.

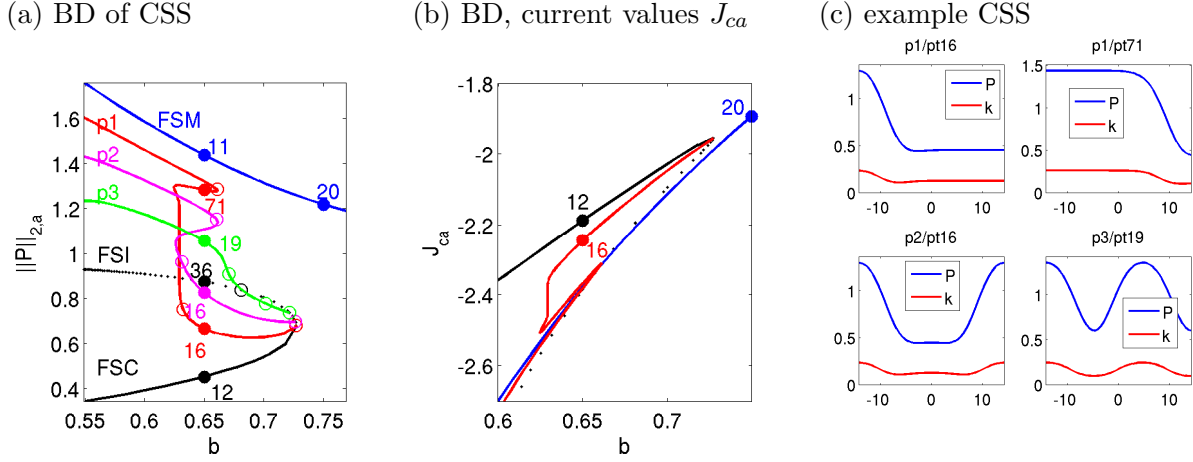


Figure 1: Example bifurcation diagrams and solution plots from running `bdcmds.m`. For  $b < b_{\text{fold}} \approx 0.73$  there are three branches of FCSS, here called FSC (Flat State Clean, low  $P$ ), FSI (Flat State Intermediate), and FSM (Flat State Muddy, high  $P$ ). On FSC/FSI there are a number of bifurcations to patterned CSS branches. The BD in  $J_{ca}$  in (b) shows that at, e.g.,  $b = 0.65$  we have  $J(\text{FSI}) < J(\text{FSM}) < J(\text{p1/pt71}) < J(\text{p1/pt16}) < J(\text{FSC})$ , suggesting the FSC to be an optimal steady state. However, this does not exclude  $\text{p1/pt16}$  or  $\text{p1/pt71}$  to be optimal steady states, and moreover, there might be a path from the FSC to some other CSS with the SPP, dominating the FSC as a CSS. See [GU15] for further discussion.

Table 3: Selected commands from the script file `bdcmds.m`. See the source code for more details, and, e.g., `bdcmds2D.m` for the quite similar commands in 2D. Note that these files are in Matlab cell-modes, and the cells should be executed one by one. In the last command, `p.fuha.con` must be set.

---

```

%% stat. BD for sloc, main script-file. First set matlab paths:
path('../p2plib',path);path('../p2poclib',path);
%% ---- Scenario 1, FSC/FSI branch
close all; p=[];lx=2*pi/0.44; ly=0.1; nx=50; ny=1; sw=1; p=slinit(p,lx,ly,nx,ny,sw);
p=setfn(p,'f1'); screenlayout(p); p=cont(p,100);
%% ---- FSM branch
sw=2; p=slinit(p,lx,ly,nx,ny,sw); p=setfn(p,'f2'); p.nc.dsmax=0.2; p=cont(p,15);
%% ---- bif from f1 (set bpt* and p* and repeat as necessary)
p=swibra('f1','bpt1','p1',-0.05); p.nc.dsmax=0.3; p.nc.neigdet=50; p=cont(p,150);
%% ---- plotting of BD, L2 and J_{ca}, and solution plots
clf(3); pcmp=3; plotbraf('f1','bpt1',3,pcmp,'lab',12,'cl','k'); % FSC (+ other branches)
clf(3); pcmp=4; plotbraf('f1','bpt1',4,pcmp,'lab',12,'cl','k'); % FSC (+other branches)
plot1Df('p1','pt16',1,1,1,2); plot1Df('p1','pt71',2,1,1,2); % solution plots ...
stancssvalf('p1','pt16'); % extract values <P>, <k>, J_{c,a} from solution in p1/pt16;

```

---

Naturally, there are some modifications to the standard `pde2path` plotting commands, see, e.g., `plot1D.m`. These work as usual by overloading the respective `pde2path` functions by putting the adapted file in the current directory. See Fig. 1 for example results of running `bdcmds`.

### 2.1.2 Canonical paths

The goal is to calculate canonical paths from some starting state  $v(0)$  to a CSS  $\hat{u}_1$  with the SPP. For this we use one of the continuation algorithm `iscnat` or `iscarc` which in turn call `mtom`, based



on TOM. Since we only wanted minimal modifications of TOM we found it convenient (though somewhat dangerous) to pass a number of parameters to the functions called by `mtom` via global variables. Thus, at the start of the canonical path scripts (here `cpdemo.m`) we define a number of global variables, see Table 4.

Table 4: Global variables for the computation of canonical paths, i.e., mainly for interfacing the driver scripts with the functions called by TOM.

name	purpose
<code>s0,s1</code>	<code>pde2path</code> structs containing the boundary values at $t = 0$ ( <code>s0</code> ) and at $t = T$ ( <code>s1</code> )
<code>Psi</code>	the matrix $\Psi$ to encode the BC at $t = T$
<code>u0, u1</code>	vectors containing the current values of $u$ at the boundaries
<code>par</code>	the parameter values from <code>s1</code> (only for convenience)
<code>um1, um2</code>	solutions at continuation steps $j - 1$ and $j - 2$ (to calculate secant predictors and used in extended system in <code>iscarc</code> )
<code>sig</code>	current (arclength) stepsize in <code>iscarc</code>

The usage of `p2poc` to compute canonical paths is best understood by inspecting and running cell-by-cell the demo file `cpdemo.m`. Some results of running `cpdemo` are shown in Fig. 2. (a) shows the “easy” case of a (canonical) path from `p3/pt19` to FSC (up to line 11), while (b) to (f) illustrate the case of a fold in  $\alpha$  when trying to get a path from `p1/pt71` to the FSC. (c)-(e) show the two paths obtained from picking two paths from the output of `iscarc` and a posteriori correcting to  $\alpha = 0.6$  (lines 24-26, only for the “upper” canonical path). Line 21 from `slcpdemo` prepares the calculation of Skiba paths, explained in §2.1.3. We now give a brief overview of the involved `p2poclib` functions, with the line-numbers referring to Table 6.

`[alv,vv,sol,udat,tlv,tv,uv]=iscnat(alvin,sol,usec,opt,fn);` (line 9)

Input: `alvin` as the vector of desired  $\alpha$  values, for instance `alvin=[0.25 0.5 1]`. `sol,usec` can be empty (typically on first call), but on subsequent calls should contain the last solution and the last secant (if `opt.msw=1`). `fn` is a structure containing the filenames for the start CSS and end CSS<sup>4</sup>, and `opt` is an options structure containing TOM options and some more, see Table 5 and Remark 2.1.

Output: `alv` as the  $\alpha$  vector of successful solves; `vv` as the canonical path values  $J_a$  of the successful solves; `sol` as the (last) canonical path; `ydat` contains the 2 last steps and the last secant (useful for repeated calls, and for using `iscnat` as startup for `iscarc`). Finally, if `opt.retsw=1`, then `tlv,tv,uv` contain data of *all* successful solves, namely: for the  $j$ -th step,  $j=1:\text{length}(\text{alv})$ , `tlv(j)`, contains the meshsize (in  $t$ ), `tv(j,1:tlv(j))` the mesh, and `uv(j,1:n,1:tlv(j))` the solution. Thus, via `sol.x=xv(j,1:tlv(j)); sol.y=squeeze(uv(j,1:n,1:tlv(j)))`; the solution of the  $j$ -th step is recovered. This is useful for a posteriori inspecting some solution from the continuation (see line 24, and `skiba.m` in `vegdemo`). Note that `uv` can be large, and might give memory problems. If `opt.retsw=0`, then `tlv,tv,uv` are empty.

`[alv,vv,usec,esol,tlv,tv,uv]=iscarc(esol,usec,opt,fn);` (line 15)

Input: as for `iscnat` (without `alvin`), but with `esol` containing the extended solution  $(u_\alpha, \alpha)$ , and similar for the secant `usec`; as in `iscnat`, if `opt.start=1`, then `esol,usec` can be empty.

Output: `alv, val`  $\in \mathbb{R}^{1 \times m}$  as the vectors of achieved  $\alpha$  and  $J_a(\alpha)$ ; `usec,esol` as the last secant/solution; `tlv,tv,uv` as in `iscnat`, but all in the sense of extended solutions, i.e.  $(u_\alpha, \alpha)$ .

<sup>4</sup>Taking  $v$  from a CSS is basically for convenience: Of course, the initial states  $v_0$  can be arbitrary, and there are no initial conditions for the co-states (and in particular those of the “start CSS” are not used). However, the construction is also motivated by the fact that one of the most interesting questions is if given  $v$  from some CSS  $\hat{u}_0$  there exists a canonical path connecting to a different CSS  $\hat{u}_1$ , and whether this yields a higher value. Then, it is of course also interesting if one can also go the other way round, and for this we provide the `flip` parameter in `setfnflip`, see below.

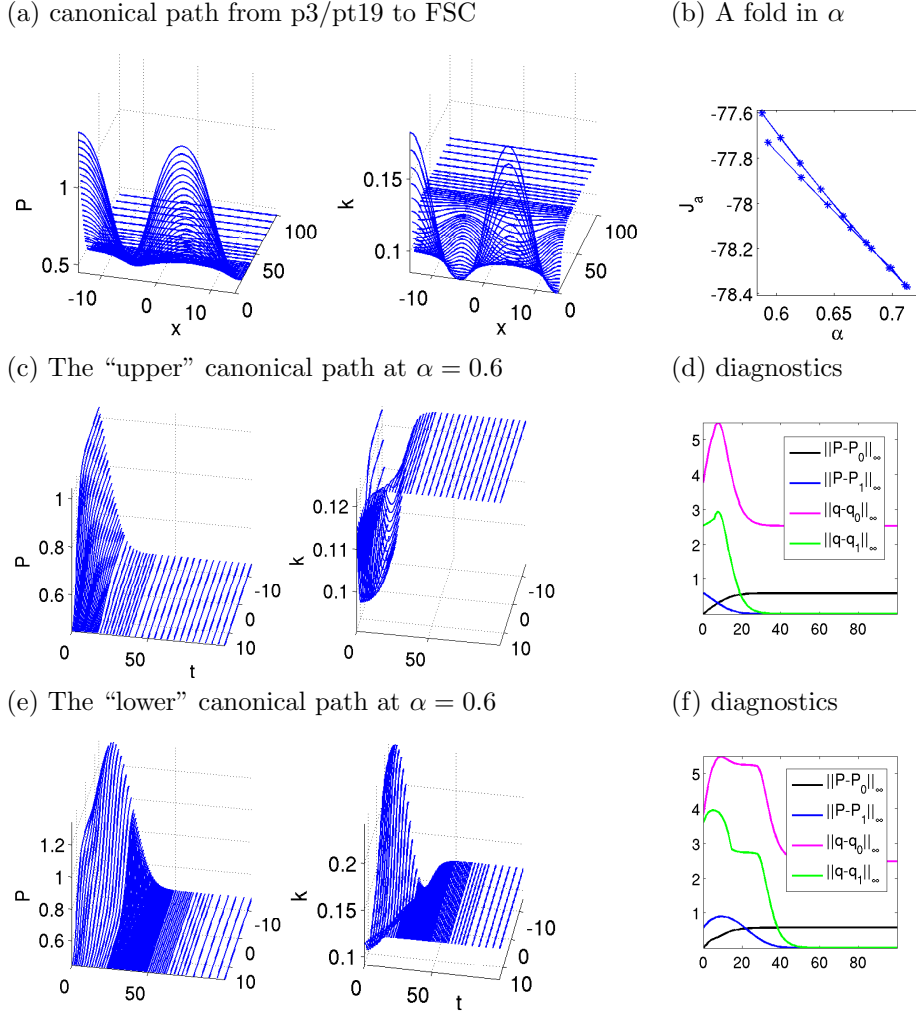


Figure 2: Example outputs from running `slcpdemo.m`

**Remark 2.1.** Concerning the original TOM options we remark that typically we run `iscnat` and `iscarc` with weak error requirements and what appears to be the fastest monitor and order options, i.e., `opt.Monitor=3`; `opt.order=2`; . Once continuation is successful (or also if it fails at some  $\alpha$ ), we can always postprocess by calling `mtom` again with a higher order, stronger error requirements, and different monitor options, e.g., mesh-refinement based on condition rather than error alone. See the original TOM documentation. ]

The functions `iscnat` and `iscarc` are the two main user interface functions for the canonical path numerics. There are a number of additional functions for internal use, and some convenience functions, which we briefly review as follows:

`[Psi,mu,d,t]=getPsi(s1)`; compute  $\Psi$ , the eigenvalues  $\mu$ , the defect  $d$ , and a suggestion for  $T$ .

Note that this becomes expensive with large  $2nN$  (i.e., the number of spatial DoF).

`[sol,info]=mtom(ODE,BC,solinit,opt,varargin)`; the ad-hoc modification of TOM, which allows for  $M$  in (10a). Extra arguments  $M$  and `lu,vsw` in `opt`. If `opt.lu=0`, then `\` is used for solving linear systems instead of an LU-decomposition, which becomes too slow when  $2nN \times m$  becomes too large. See the TOM documentation for all other arguments including `opt`, and note that the modifications in `mtom` can be identified by searching “HU” in `mtom.m`. Of course `mtom` (as any other function) can also be called directly (line 26), which for instance is useful to postprocess the output of some continuation by changing parameters by hand.

Table 5: Switches/controls in `opt` besides the TOM options. Note that `iscarc` only has a very elementary stepsize control via `opt.sigmin, opt.sigmax`.

name	purpose	name	purpose
<code>start</code>	1 for startup, 0 else	<code>M,lu,vsw</code>	mass matrix, lu-switch and (extra) verbosity for <code>mtom</code>
<code>retsw</code>	1 to return full continuation data	<code>t1</code>	truncation time $T$
<code>rhoi</code>	index of $\rho$ in <code>par</code>	<code>tv</code>	current $t$ -mesh
<code>nti</code>	# of points in startup $t$ -mesh	<code>sigmin, sigmax</code>	min&max stepsize for <code>iscarc</code>
<code>nsteps</code>	number of steps for <code>iscarc</code>		

Table 6: Selected commands from the script file `cpdemo.m`. See the source code for more details and, e.g., more fancy plotting.

```

1 % driver script for Shallow Lake Optimal Control, first set paths and globals
2 path('../tom',path); path('../p2poclib',path);
3 close all; clear all; global s0 s1 u0 u1 Psi par xi ym1 ym2 sig;
4 %% Preparations: put filenames into fn, set some bvp parameters
5 sd0='f1'; sp0='pt12'; sd1='p3'; sp1='pt19'; flip=1; % p3->FSC
6 fn=setfnflip(sd0,sp0,sd1,sp1,flip); opt=[]; opt=ocstanopt(opt);
7 opt.rhoi=1; opt.t1=100; opt.start=1; opt.tv=[]; opt.nti=10; opt.retsw=0;
8 %% the solve and continue call, and some plots
9 sol=[]; alvin=[0.1 0.25 0.5 0.75 1]; v=[15,30];
10 [alv,vv,sol,ydat,tlv,xv,yv]=iscnat(alvin,sol,[],opt,fn); slsolplot(sol,v);
11 %% ---- A fold in alpha, here iscarc needed. Prep. and initial iscarc call
12 sd0='f1'; sp0='pt12'; sd1='p1'; sp1='pt71'; flip=1; fn=setfnflip(sd0,sp0,sd1,sp1,flip);
13 esol=[]; ysec=[]; opt.nsteps=3; opt.alvin=[0.2 0.25]; sig=0.1; opt.nti=10; opt.tv=[];
14 opt.Stats_step='on'; opt.start=1; opt.sigmax=1; opt.retsw=1;
15 [alv,vv,ysec1,esol1,tlv,xv,yv]=iscarc(esol,ysec,opt,fn); opt.start=0;
16 %% subsequent icarc-calls (repeat this cell)
17 opt.nsteps=20; ysec=ysec1; esol=esol1; % new input (for repeated calls)
18 [alv1,vv1,ysec1,esol1,tlv1,xv1,yv1]=iscarc(esol,ysec,opt,fn);
19 alv=[alv alv1]; vv=[vv vv1]; tlv=[tlv tlv1]; xv=[xv xv1]; yv=[yv yv1];
20 %% Postprocess sol from iscarc, first a simple plot of J over alpha
21 alv0=alv; vv0=vv; xv0=xv; yv0=yv; tlv0=tlv; % save results for skibademo.m
22 figure(6); clf; plot(alv(1,:),vv(1,:),'-*'); xlabel('\alpha'); ylabel('J_{\alpha}');
23 %% fix al from iscarc to some given value and compute CPs, first j=22, then j=34
24 j=22; tl=tlv(j); n=s1.nu; sol.x=xv(j,1:tlv(j)); sol.y=squeeze(yv(j,1:n,1:tlv(j)));
25 al=0.6; u0=al*s0.u(1:n)+(1-al)*s1.u(1:n); u1=s1.u(1:s1.nu);
26 opt.M=s1.mat.M; sol=mtom(@mrhs,@cbcf,sol,opt); v=[100,30]; slsolplot(sol,v);

```

`f=mrhs(t,u,k)`; `J=fjac(t,u)`; and `f=mrhse(t,u,k)`; `J=fjace(t,u)`; the `rhs` and its Jacobian to be called within `mtom`. These are just wrappers which calculate  $f$  and  $J$  by calling the resp. functions in the `pde2path`-struct `s1`, which were already set up and used to calculate the CSS. `s1` is passed as a global variable. Similar remarks apply to `mrhse` and `fjace` for the extended setting in `iscarc`.

`bc=cbcf(ya,yb)`; `[ja,jb]=cbcjac(ya,yb)` and `bc=cbcfе(ya,yb)`; `[ja,jb]=cbcjace(ya,yb)`; The boundary conditions (in time) for (10) and the associated Jacobians. Implemented by passing  $u_0, \hat{u}_1, \Psi$  and similar globally. The `*e` (as in extended) versions are for `iscarc`.

`jcaval=jcai(s1,sol,rho)` and `djca=isjca(s1,sol,rho)`; Calculate the objective value

$$J(u) = \int_0^T e^{-\rho t} J_{ca}(v(t,\cdot), k(t,\cdot)) dt \quad (23)$$

of the solution  $u$  in `sol` (with  $J_c$  taken from `s1.fuha.jcf`), and similarly the discounted value of a CSS contained in `sol.y(:,end)`.

`fn=setfnflip(sd0,sp0,sd1,sp1,flip)`; generate the filename struct `fn` from `sd0`, `sp0` (`sd0/sp0.mat` contains IC  $u_0$ ) and `sd1,sp1` (contains  $\hat{u}$ ); if `flip=1`, then interchange `*0` and `*1`.  
`psol3D(p,sol,wnr,cmp,v,tit)`;  $x-t$  plots of canonical paths; plot component `cmp` of a canonical path `sol` to figure `wnr`, with view `v` and title `tit`. If `cmp=0`, then plot the control `k`, extracted from `sol` via `p.fuha.con`.

Thus, after having set up `p` as in §2.1.1 for the CSS, including  $G$  and `p.fuha.jcf`, the user does not need to set up any additional functions to calculate canonical paths and their values. However, typically there are some functions which should be adapted to the given problem, e.g., for plotting, for instance

`slsolplot(sol,v)`; (line 10) which calls:

`zdia=sldiagn(sol,wnr)`; Plot some norms on a canonical path as functions of  $t$  to figure(`wnr`).

This is for instance useful to check the convergence behaviour of the canonical path as  $t \rightarrow T$ , cf. (d),(f) in Fig. 2.

### 2.1.3 A patterned Skiba point

In ODE OC applications, if there are several locally stable OSS, then often an important issue is to identify their domains of attractions. These are separated by so called threshold or Skiba-points (if  $N = 1$ ) or Skiba-manifolds (if  $N > 1$ ), see [Ski78] and [GCF<sup>+</sup>08, Chapter 5]. Roughly speaking, these are initial states from which there are several optimal paths with the same value but leading to different CSS. In PDE applications, even under spatial discretization with moderate  $nN$ , Skiba manifolds should be expected to become very complicated objects. Thus, here we just give one example for the SLOC model how to compute a patterned Skiba point between FSC and FSM.

In Line 17-19 of `cpdemo.m` we attempt to find a path from  $P_{PS}$  given by `p1/pt71` to  $(P,q)_{FSC}$  given by `FSC/pt12`; this fails due to the fold in  $\alpha$ . However, for given  $\alpha$  we can also try to find a path from the initial state  $P_\alpha(0) := \alpha P_{PS} + (1 - \alpha)P_{FSC}$  to the FSM, and compare to the path to the FSC. For this, in line 21 of `cpdemo.m`, we stored the  $\alpha$  and  $J_{ca}$  values into `alv0`, `vv0`, and also the path data into `tlv0, tv0 uv0`. See `skibademo.m` in Table 7 (in particular line 11 and the following) how to put the values `uv0(j, :, 1)` into `s0` and subsequently find the paths to the FSM, and Fig. 3 for illustration.

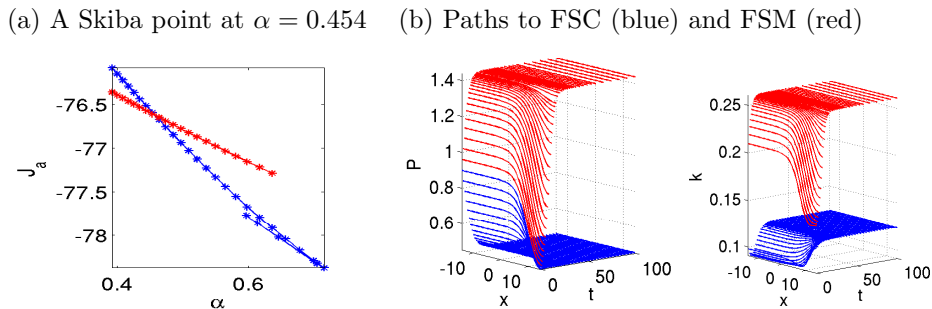


Figure 3: Example outputs from `skibademo.m`

### 2.1.4 Further comments

The files `bdcmds.m` and `cpdemo.m` also contain some of the commands used to study Scenario 2, see [Gra15] for discussion of related results obtained via `OCMat`. Moreover, the directory `slocdemo` contains the script files `bdcmds2D.m` and `cpdemo2D.m`, used to compute CSS and canonical paths for (22) over the 2D domain  $\Omega = (-L, L) \times (-\frac{L}{2}, \frac{L}{2})$  (based on exactly the same init file `slinit.m`), some auxiliary plotting functions `plotsolf.m` and `plotsolfu.m`, and the function `sol2mov.m` used

Table 7: The script file `skibademo.m`. See text for comments.

---

```

1 % Skiba example, continues cpdemo.m
2 % find paths from the yv0 initial states from cpdemo.m to FSM
3 js=10; je=30; jl=js-je+1; % alpha-range; now set the target and Psi to FSM:
4 s1=loadp('f2','pt11'); u1=s1.u(1:s1.nu); [Psi,muv,d,t1]=getPsi(s1);
5 a0l=length(alv0); tva=zeros(jl,opt.Nmax+1); % some prep. and fields to hold paths
6 uva=zeros(jl,n+1,opt.Nmax+1); alva=[]; vva=[]; tav1=[]; sol=[];
7 alvin=[0.1 0.25 0.5 0.75 1]; % we run from uv0(j,:) to FSM with iscnat
8 tv=linspace(0,opt.t1,opt.nti); se=2; opt.tv=tv.^se./opt.t1^(se-1); doplot=1;
9 opt.msw=0; opt.Stats_step='off'; v=[50,8]; % switch off stats
10 for j=js:je;
11     fprintf('j=%i, al=%g\n', j, alv0(j)); s0.u(1:n)=uv0(j,1:n,1)';
12     [alv,vv,sol,udat]=iscnat(alvin,[],[],opt,fn);
13     if alv(end)==1; Jd=vv0(j)-vv(end); fprintf('J1-J2=%g\n',Jd); % contin. successful
14         alva=[alva alv0(j)]; vva=[vva vv(end)]; tl=length(sol.x); % put vals in vector
15         tav1=[tav1 tl]; tva(j,1:tl)=sol.x; uva(j,1:n,1:tl)=sol.y;
16         if abs(Jd)<0.05; doplot=asknu('plot path?',doplot); % Skiba point(s) found
17             if doplot==1; sol0=[]; alp=alv0(j); % plot the paths to FSC and FSM
18                 sol0.x=tv0(j,1:tlv0(j)); sol0.y=squeeze(uv0(j,1:n,1:tlv0(j)));
19                 psol3Dm(s1,sol0,sol,1,1,[]); view(v); xlabel('P'); pause
20             end
21         end
22     end
23 end
24 %% plot value diagram
25 figure(6); plot(alv0(js:jep),vv0(js:jep),'-*b'); hold on; plot(alva,vva,'-r');
26 xlabel('\alpha', 'FontSize',s1.plot.fs); ylabel('J_{a}', 'FontSize',s1.plot.fs);

```

---

to generate movies of canonical paths. See, e.g., [GU15, Fig. 4,5] for some results, while some movies can be downloaded at the `pde2path` homepage.

## 2.2 The vegOC model

Our second example, from [Uec15], concerns the optimal control of a reaction diffusion *system* used to model grazing in a semi arid system for biomass (vegetation)  $v$  and soil water  $w$ , following [BX10]. Here, semi arid means that there is enough water to support *some* vegetation, but not enough water for a dense homogeneous vegetation. This is an important problem as overgrazing in semi arid areas often is a serious threat that may lead to irreversible desertification, see, e.g., [SBB<sup>+</sup>09], and the references therein.

Denoting the harvesting (grazing) effort as the control by  $E$ , we consider

$$V(v_0, w_0) = \max_{E(\cdot, \cdot)} J(v_0, w_0, E), \quad (24a)$$

$$\partial_t v = d_1 \Delta v + [gwp^\eta - d(1 + \delta v)]v - H, \quad (24b)$$

$$\partial_t w = d_2 \Delta w + R(\beta + \xi v) - (r_u v + r_w)w, \quad (24c)$$

with harvest  $H = v^\alpha E^{1-\alpha}$ , and current value objective function  $J_c = J_c(v, E) = pH - cE$ , which thus depends on the price  $p$ , the costs  $c$  for harvesting/grazing, and  $v, E$  in a classical Cobb–Douglas form with elasticity parameter  $0 < \alpha < 1$ . For the modeling, and the meaning and values of the parameters ( $g, \eta, d, \delta, \beta, \xi, r_u, r_w, d_{1,2}$ ) we refer to [BX10, Uec15] and the references therein (see also Table 8, line 9 for the parameter values), and here only remark that  $\rho = 0.03, p = 1.1, \alpha = 0.3, c = 1$  are the economic parameters, and we take the rainfall  $R$  as the main bifurcation parameter. Fur-

thermore, we have the BC and IC

$$\partial_\nu v = \partial_\nu w = 0 \text{ on } \partial\Omega, \quad (v, w)|_{t=0} = (v_0, w_0). \quad (24d)$$

Denoting the co-states by  $(\lambda, \mu)$  we have the local current value Hamiltonian

$$\begin{aligned} \mathcal{H}(v, w, \lambda, \mu, E) = & J_c(v, E) + \lambda [d_1 \Delta v + (gwp^\eta - d(1 + \delta v))v - H] \\ & + \mu [d_2 \Delta w + R(\beta + \xi v) - (r_u v + r_w)w], \end{aligned} \quad (25)$$

and obtain the canonical system

$$\partial_t v = \mathcal{H}_\lambda = d_1 \Delta v + [gwp^\eta - d(1 + \delta v)]v - H, \quad (26a)$$

$$\partial_t w = \mathcal{H}_\mu = d_2 \Delta w + R(\beta + \xi v) - (r_u v + r_w)w, \quad (26b)$$

$$\begin{aligned} \partial_t \lambda = \rho \lambda - \mathcal{H}_v = & \rho \lambda - p\alpha v^{\alpha-1} E^{1-\alpha} - \lambda [g(\eta + 1)wv^\eta - 2d\delta v - d - \alpha v^{\alpha-1} E^{1-\alpha}] \\ & - \mu (R\xi - r_u)w - d_1 \Delta \lambda, \end{aligned} \quad (26c)$$

$$\partial_t \mu = \rho \mu - \mathcal{H}_w = \rho \mu - \lambda g v^{\eta+1} + \mu (r_u v + r_w) - d_2 \Delta \mu, \quad (26d)$$

where  $E$  is obtained from solving  $\partial_E \mathcal{H} = 0$ , giving

$$E = \left( \frac{c}{(p - \lambda)(1 - \alpha)} \right)^{-1/\alpha} v. \quad (26e)$$

With the notation  $u = (v, w, \lambda, \mu)$ , the IC, the BC, and the transversality condition are

$$(v, w)|_{t=0} = (v_0, w_0), \quad \partial_\nu u = 0 \text{ on } \partial\Omega, \quad \lim_{t \rightarrow \infty} e^{-\rho t} u(t) = 0. \quad (26f)$$

To study (26), we write it as  $\partial_t u = -G(u)$  and basically need to set up  $G$  and the BC. This follows the general `pde2path` settings with the OC related modifications already explained in §2.1, and thus we only give the following remarks, first concerning `veginit.m`, see Table 8.

In line 2 we only set up `p.fuha.sG` since in this demo we use `p.sw.jac=0` (numerical Jacobians), and hence do not need to set `p.fuha.sGjac`.

lines 4-7 set the Neumann BC and diffusion tensor for the 4 component system (see `gnbc.m` and `isoc.m` for documentation)

lines 8-10 set the desired  $R$  values for output of CSS to disk, the parameter values, and the main bifurcation parameter. Of course, one could also hard-code all parameters except  $R$ , but we generally recommend to treat parameters as parameters since this is needed if later a continuation in some other parameter is desired, and since it usually makes the code more readable.

Table 8: Selected commands from the init-routine `veginit.m`. See the source code for more details.

---

```

1 function p=veginit(p,lx,ly,nx,ny,sw,rho) % init-routine for vegOC
2 p=stanparam(p); p.nc.neq=4; p.fuha.sG=@vegsG; p.fuha.jcf=@vegjcf; p.fuha.outfu=@ocbra;
3 p.mesh.geo=rec(lx,ly); p=stanmesh(p,nx,ny); p.sol.xi=0.005/p.np; % generate mesh
4 q=zeros(p.nc.neq); g=zeros(p.nc.neq,1); % setting up Neumann BC for 4 components
5 bc=gnbc(p.nc.neq,4,q,g); p.fuha.bc=@(p,u) bc; p.fuha.bcjac=@(p,u) bc;
6 p.d1=0.05; p.d2=10; p.eqn.a=0; p.eqn.b=0; % setting up K for 4 components
7 c=diag([p.d1, p.d2, -p.d1, -p.d2]); p.eqn.c=isoc(c,4,1);
8 p.usrlam=[4 10 20 26 28]; % desired R values for output of CSS
9 par=[rho 1e-3 0.5 0.03 0.005 0.9 1e-3 34 0.01 0.1 1 1.1 0.3]; % par-values
10 p.nc.ilam=8; % choose the active par, here Rainfall R
11 % now continue with setting a few more param and the initial guess ... see veginit.m

```

---

Table 9: Implementation of the rhs  $G$  and  $J_c$  for (26), and the aux function  $\text{efu}$ .

---

```

1 function r=vegsG(p,u) % rhs for veg0C problem
2 par=u(p.nu+1:end); rho=par(1); g=par(2); eta=par(3); % extract param
3 d=par(4); del=par(5); beta=par(6); xi=par(7); rp=par(8); up=par(9); rw=par(10);
4 cp=par(11); pp=par(12); al=par(13); [e,h,J]=efu(p,u); % calculate H
5 v=u(1:p.np); w=u(p.np+1:2*p.np); % extract soln-components, states
6 l1=u(2*p.np+1:3*p.np); l2=u(3*p.np+1:4*p.np); % co-states
7 f1=(g*w.*v.^eta-d*(1+del*v)).*v-h; f2=rp*(beta+xi*v)-(up*v+rw).*w; % f1,f2
8 f3=rho*l1-pp*al*h./v-l1.*(g*(eta+1)*w.*v.^eta-2*d*del*v-d-al*h./v)-l2.*(rp*xi-up*w);
9 f4=rho*l2-l1.*(g*v.^(eta+1))-l2.*(-up*v-rw); f=[f1;f2;f3;f4];
10 r=p.mat.K*u(1:p.nu)-p.mat.M*f; % the residual

```

---

```

1 function jc=vegjcf(p,u); [e,h,jc]=efu(p,u); % J_c for veg0C, here just an interface

```

---

```

1 function [e,h,J]=efu(p,varargin) % extract [e,h,J] from p or u
2 if nargin>1 u=varargin{1}; else u=p.u; end
3 par=p.u(p.nu+1:end); cp=par(11); pp=par(12); al=par(13);
4 v=u(1:p.np); l1=u(2*p.np+1:3*p.np);
5 gas=((pp-l1)*(1-al)./cp).^(1/al); e=gas.*v; h=v.^al.*e.^(1-al);
6 J=pp*v.^al.*e.^(1-al)-cp*e;

```

---

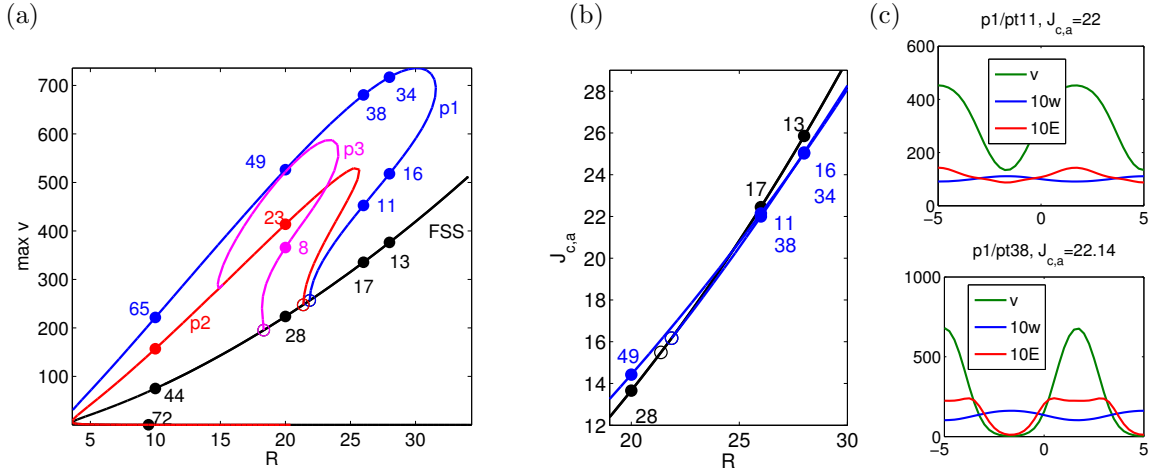


Figure 4: Outputs of `bd1ddemo.m`. (a),(b) bifurcation diagrams of CSS in 1D; (c) example solutions.

Table 9 shows the complete codes for setting up  $G$  and the current value  $J_c$ . Both use the auxiliary function `efu`, which is also used in, e.g., `valf.m` to tabulate characteristic values of CSS.

Figure 4 shows a basic bifurcation diagram of CSS in 1D with  $\Omega = (-L, L)$ ,  $L = 5$ , from the script file `vegbd1d.m`, which follows the same principles as the one for the SLOC demo. The blue branch in (a) represents the primary bifurcation of PCSS, which for certain  $R$  have the SPP, and moreover, are POSS. See also [Uec15] for more plots, including a comparison with the uncontrolled case of so called “private optimization”, and 2D results for  $\Omega = (-L, L) \times (-\sqrt{3}L/2, \sqrt{3}L/2)$  yielding various POSS, including hexagonal patterns.

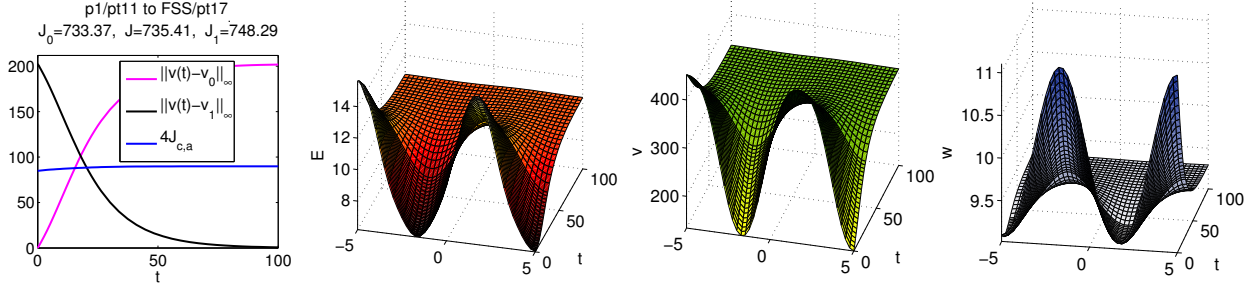
The script files `vegcpdemo.m` for canonical paths, and `vegskiba.m` for a Skiba point between the flat optimal steady state  $FSS/pt13$  and the POSS  $p1/pt34$ , again follow the same principles as in the the SLOC demo. See Figures 5, and 6 for example outputs, and [Uec15] for a detailed discussion. In a nutshell, we find that:

- (a) For large  $R$  the FCSS is the unique CSS of (26), and is optimal, hence a globally stable FOSS (Flat Optimal Steady State).
- (b) For smaller  $R$  there are branches of (locally stable) POSS (Patterned Optimal Steady States),

which moreover dominate all other CSS.

- (c) For the uncontrolled problem, Flat Steady States (FSS) only exist for much larger  $R$  than the FCSS under control.
- (d) At equal  $R$ , the profit  $J$  (or equivalently the discounted value  $J_c/\rho$ ) of the uncontrolled FSS is much lower than the value of the FCSS under control.

(a)  $R = 26$ , the canonical path from the lower PCSS(p1/pt11) to the FCSS (FSS/pt17)



(b)  $R = 26$ , the canonical path from the FCSS to the upper PCSS (p1/pt38)

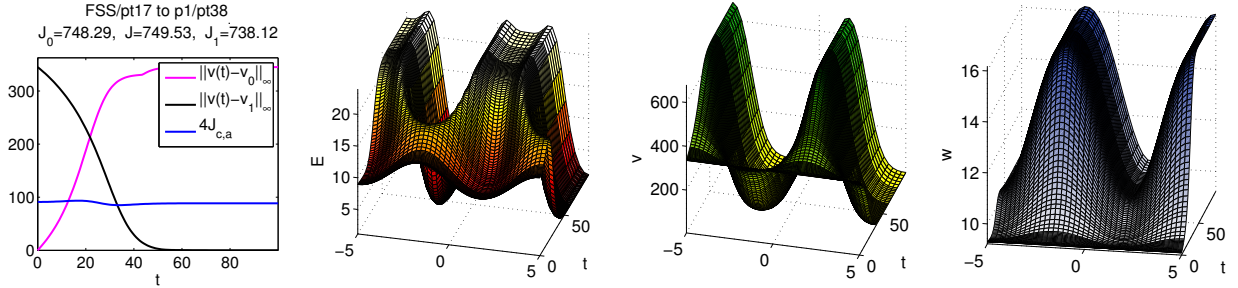


Figure 5: Example output of `vegcpdemo.m`: Two canonical paths. The leftmost panels indicate the convergence behaviour, the current value profits, and obtained objective values. The middle and right panels show the strategy  $E$  and the corresponding behaviour of  $(v, w)$ . See [Uec15] for comments and more details.

(a) A Skiba point at  $\alpha \approx 0.9$  (b) Paths of (almost) equal values to the FCSS and the upper PCSS.

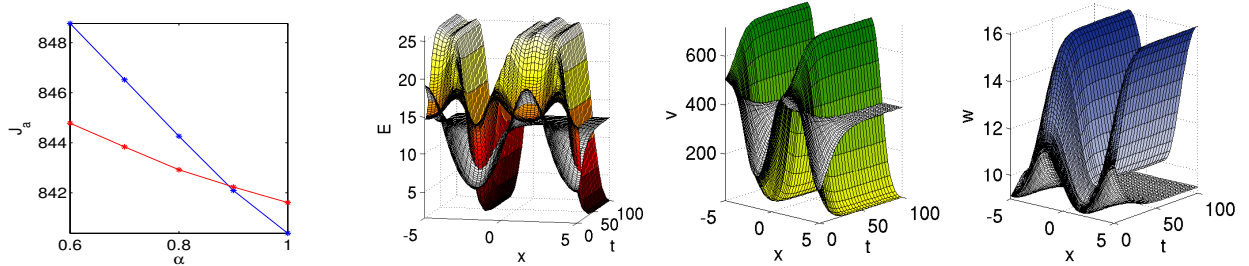


Figure 6:  $R = 28$ , example outputs from `skibademo.m`. In (a), the blue line gives  $J$  for the canonical path  $t \mapsto u(t)$  from  $(v, w)_\alpha(0) := \alpha(v, w)_{PS} + (1 - \alpha)(v, w)_{FSS}$ , where FSS denotes FSS/pt13, and PS denotes p1/pt16. The red line gives  $J$  for the CP  $t \mapsto \tilde{u}(t)$  from  $P_\alpha(0)$  to the upper PCSS p1/pt34. Similarly, the white surfaces in (b) are for  $u$  and the colored ones for  $\tilde{u}$ .  $R = 28$ .

### 3 Using OOPDE

Setting up a 1D interval  $(-l_x, l_x)$  as a thin strip  $(-l_x, l_x) \times (-\delta_y, \delta_y)$  is convenient, but not elegant and not efficient. Therefore we started linking `pde2path` with the free Matlab FEM package



OOPDE ([www.mathe.tu-freiberg.de/nmo/mitarbeiter/uwe-pruefert/software](http://www.mathe.tu-freiberg.de/nmo/mitarbeiter/uwe-pruefert/software)) for 1D, 2D and 3D problems, which in most interfaces mimicks the `pdetoolbox`. This is very much work in progress, but nevertheless here we explain the basic usage OOPDE for 1D and 2D problems, where so far we only provide a standard setup for OOPDE for the semilinear case treated otherwise via `sfem=1`, and, for instance, no mesh-adaptation yet. As also OOPDE is currently under heavy development, together with `p2poc` we provide a “light” version OOPDElight with basic functionality in 1D and 2D.

To use OOPDE, there are essentially two new m-files in `p2plib`, namely `stanpdeo1D.m` and `stanpdeo2D.m`, which create very basic OOPDE objects, and hence should be seen as templates for creating more sophisticated OOPDE objects. Basically, `pdeo=stanpdeo1D(lx,h)` just sets the grid `pdeo.grid` on the interval  $(-l_x, l_x)$  with mesh-size  $h$ , and the desired FEM class `pdeo.fem`, by default `pdeo.fem=lagrange11D`. Similarly, `pdeo=stanpdeo2D(lx,ly,h)` sets the grid on the rectangle  $(-l_x, l_x) \times (-l_y, l_y)$  with mesh-size  $h$ , and `pdeo.fem=lagrange12D`.

To explain the differences to the old `pde2path` setup we refer to files in the directories `oosloc` and `oovegoc`, which by setting some switches can be used to compare the `pdetoolbox` and the OOPDE settings. The driver scripts in `oosloc` are `bdcmds*.m`, `cpdemo*.m` (1D and 2D) and `skibademo.m`, and those in `oovegoc` are `bd1d.m` and `vegcpdemo.m` (only 1D). Table 10 shows (parts of) `slinit.m`, which is used in the script files `bdcmds*.m` as `p=slinit(p,lx,ly,nx,ny,sw,ndim,oo)`.

Table 10: The init routine `slinit.m`, called by `cmds*.m` with switch `oo=1,0` to use OOPDE or not.

```

1 function p=slinit(p,lx,ly,nx,ny,sw,ndim,oo) % init-routine
2 p=stanparam(p); p.nc.neq=2; p.fuha.G=@slf; p.fuha.Gjac=@sljac; p.fuha.outfu=@ocbra;
3 p.fuha.sG=@slsG; p.fuha.sGjac=@slsGjac; p.fuha.jcf=@sljcf; p.fuha.con=@slcon;
4 if oo==0 % use pdetool
5     if ndim==1; ny=1; ly=lx/nx; p.plot.pstyle=4; end % quasi 1D setup
6     [p.mesh.geo,bc]=recnbc2(lx,ly); p=stanmesh(p,nx,ny);p=setbmesh(p); % mesh
7     p.fuha.bc=@(p,u) bc; p.fuha.bcjac=@(p,u) bc; % Neumann BC
8     p.eqn.c=[1;0;0;1;-1;0;0;-1]; p.eqn.a=0; p.eqn.b=0; % c,a,b tensors
9     p.sw.sfem=1; p.vol=4*lx*ly;
10 else; h=2*lx/nx; % use OOPDE
11     if ndim==1; pdeo=stanpdeo1D(lx,h); p.vol=2*lx;
12     else pdeo=stanpdeo2D(lx,ly,h); p.vol=4*lx*ly; end
13     p.oopde=pdeo; p.np=pdeo.grid.nPoints; p.sw.sfem=-1;
14 end
15 p=setfemops(p); % from here on NO MORE DIFFERENCES between OOPDE and pdetool

```

If `oo=0`, then we use the old setup, where the parameter `ndim=1,2` is only used for convenience (line 5). If `oo=1`, then we generate an OOPDE `pde`-object `pdeo`, which in l13 we put into `p.oopde`, and set `p.sw.sfem=-1` to signal the use of OOPDE. Thus, the grid now is in `p.oopde.grid` instead of `p.mesh`, which no longer exists in the OOPDE setting. To ensure compatibility between the `oo=0` and `oo=1` approaches, instead of directly referring to `p.mesh` or `p.oopde.grid` we now use the function `[po,tr,ed]=getpte(p)`, which extracts the mesh-data as appropriate. See also Remark 3.1 on this. A final adjustment in case `oo=1` is hidden in the call to `setfemops` in line 15. There, if `p.sw.sfem < 0`, then the system matrices  $K, M$  etc are not assembled from the tensors `p.eqn.c` etc, but are generated by calls to OOPDE routines put into a function `oosetfemops.m`, for which the user is responsible; see Table 11 for the SLOC example, which is particularly simple due to the homogeneous Neumann BC. No further adaptations are needed by the user to freely switch between the `pdetoolbox` and OOPDE settings.

The results for the `oo=1` setting (with a genuine 1D domain) are identical to the `oo=0` setting (with the domain a thin strip), except that the point-labels occasionally differ slightly. However, in particular for the computation of canonical paths the `oo=1` setup runs *much* faster. This becomes even more prominent in the `oo=1` setting for the `vegOC` model in directory `oovegoc`.

Table 11: The setup routine of the FEM matrices for the SLOC model in the oo=1 setting. K and M in line 2 correspond to the scalar Laplacian and mass matrix, respectively, and are therefore extended to the two-component canonical system in line 3.

```

1 function p=ooSetfemops(p) % for SLOC, i.e., in SLOC-dir, since highly problem dependent
2 [K,M,~]=p.oopde.fem.assema(p.oopde.grid,1,1,1); % scalar K and M
3 p.mat.K=kron([[1,0];[0,-1]],K); p.mat.M=kron([[1,0];[0,1]],M); % extend to system
4 p.mat.Kadv=0; p.mat.bcG=zeros(p.nu,1); % no convection, zero RHS for the zero-flux BC

```

**Remark 3.1.** In the present setting, after assembling K, M, Kadv and bcG, we could in principle copy `p.oopde.grid` to `p.mesh` and delete the `oopde` object. However, we keep `p.oopde` for “upward compatibility”, i.e., to later use more of OOPDE, in particular as OOPDE is also our choice to implement a 3D version of `pde2path`, and in future versions of `pde2path` in 2D can be used to fully replace the `pdetoolbox`. ]

## 4 Summary and outlook

With `p2poc` we provide a toolbox to study OC problems of class (1) in a simple and convenient way, in 1D and 2D. The class (1) is quite general, and with the `pde2path` machinery we have a rather powerful tool to study the bifurcations of CSS. The computation of canonical paths is comparatively more involved. Essentially, our step (b) implements for the class (1) (parts of) the methods explained for ODE problems in [GCF<sup>+</sup>08, Chapter 7], and implemented in `OCMat` [orcos.tuwien.ac.at/research/ocmat\\_software/](http://orcos.tuwien.ac.at/research/ocmat_software/), see also [Gra15] for an extension of `OCMat` to 1D systems of class (1). In a somewhat more general sense, step (b) is a special case (for PDEs) of the “connecting orbit method”. See [DCF<sup>+</sup>97, BPS01] and the references therein for earlier work on connecting orbits in ODE problems, including connecting orbits to periodic solutions, which for ODE OC problems may also be important as long-run optimal solutions, again cf. [GCF<sup>+</sup>08]. Our setup for (b) is reasonably fast for up to 4000 degrees of freedom of  $u$  at fixed time, e.g., 1000 spatial discretization points and 4 components, and up to 200 temporal discretization points, i.e., for these values a continuation step in the calculation of a canonical path takes about a minute on a desktop computer (Intel i7, 2.3GHz).

Of course, there is a rather large number of issues we do not address (yet). Besides periodic long-run optimal solutions, one of these are state or control inequality constraints that frequently occur in OC problems. For instance, in the SLOC model we need non-negativity of  $P$  and  $k$ , and similarly we need  $v, w, E \geq 0$  in the vegOC model. In our examples we simply checked these constraints a posteriori and found them to be always fulfilled, i.e., *inactive* (which is clear in the SLOC model due to the term  $\ln k$  in  $J_c$ , but it is not clear a priori in the vegOC model). If such constraints become *active* the problem becomes much more complicated.

Clearly, it is tempting to recombine steps (a) and (b) again, at least for specific purposes. One example would be the continuation of canonical paths in a parameter  $\eta$ . Naively, this could be done “by hand” by using a canonical path  $u(\cdot, \eta)$  between  $v_0$  (or  $v_0(\eta)$ ) and  $\hat{u}(\eta)$  as an initial guess for a canonical path  $u(\cdot, \eta + \delta)$  between  $v_0$  (or  $v_0(\eta + \delta)$ ) and  $\hat{u}(\eta + \delta)$ , at the parameter value  $\eta + \delta$ . This, however, does not directly allow to check for bifurcations of canonical paths, and, perhaps more importantly, requires the recalculation of  $\Psi$  at each new  $\hat{u}(\eta)$ . See [BPS01, Pam01] for the “boundary corrector method” as an approach to avoid the latter, and, moreover, for continuation methods in the full t-BVP that for instance also allow the computation of Skiba-curves (cf. §2.1.3) in 0D, cf. also [GCF<sup>+</sup>08, §7.7–§7.8].

## References

- [AAC11] S. Anița, V. Arnăutu, and V. Capasso. *An introduction to optimal control problems in life sciences and economics*. Birkhäuser/Springer, New York, 2011.
- [ACKLT13] S. Anița, V. Capasso, H. Kunze, and D. La Torre. Optimal control and long-run dynamics for a spatial economic growth model with physical capital accumulation and pollution diffusion. *Appl. Math. Lett.*, 26(8):908–912, 2013.
- [ADS14] N. Apreutesei, G. Dimitriu, and R. Strugariu. An optimal control problem for a two-prey and one-predator model with diffusion. *Comput. Math. Appl.*, 67(12):2127–2143, 2014.
- [BPS01] W.J. Beyn, Th. Pampel, and W. Semmler. Dynamic optimization and Skiba sets in economic examples. *Optimal Control Applications and Methods*, 22(5–6):251–280, 2001.
- [BX08] W.A. Brock and A. Xepapadeas. Diffusion-induced instability and pattern formation in infinite horizon recursive optimal control. *Journal of Economic Dynamics and Control*, 32(9):2745–2787, 2008.
- [BX10] W. Brock and A. Xepapadeas. Pattern formation, spatial externalities and regulation in coupled economic–ecological systems. *Journal of Environmental Economics and Management*, 59(2):149–164, 2010.
- [CPB12] C. Camacho and A. Pérez-Barahona. Land use dynamics and the environment. Documents de travail du Centre d’Economie de la Sorbonne, 2012.
- [DCF+97] E. Doedel, A. R. Champneys, Th. F. Fairgrieve, Y. A. Kuznetsov, Bj. Sandstede, and X. Wang. AUTO: Continuation and bifurcation software for ordinary differential equations (with HomCont). <http://cmvl.cs.concordia.ca/auto/>, 1997.
- [DRUW14] T. Dohnal, J. Rademacher, H. Uecker, and D. Wetzel. pde2path 2.0. In H. Ecker, A. Steindl, and S. Jakubek, editors, *ENOC 2014 - Proceedings of 8th European Nonlinear Dynamics Conference*, ISBN: 978-3-200-03433-4, 2014.
- [GCF+08] D. Grass, J.P. Caulkins, G. Feichtinger, G. Tragler, and D.A. Behrens. *Optimal Control of Nonlinear Processes: With Applications in Drugs, Corruption, and Terror*. Springer Verlag, 2008.
- [Gra15] D. Grass. From 0D to 1D spatial models using OCMat. Technical report, ORCOS, 2015.
- [GU15] D. Grass and H. Uecker. Optimal management and spatial patterns in a distributed shallow lake model. Preprint, 2015.
- [KW10] T. Kiseleva and F.O.O. Wagener. Bifurcations of optimal vector fields in the shallow lake system. *Journal of Economic Dynamics and Control*, 34(5):825–843, 2010.
- [MS02] F. Mazzia and I. Sgura. Numerical approximation of nonlinear BVPs by means of BVMS. *Applied Numerical Mathematics*, 42(1–3):337–352, 2002. Numerical Solution of Differential and Differential-Algebraic Equations, 4-9 September 2000, Halle, Germany.
- [MST09] F. Mazzia, A. Sestini, and D. Trigiante. The continuous extension of the B-spline linear multistep methods for BVPs on non-uniform meshes. *Applied Numerical Mathematics*, 59(3–4):723–738, 2009.
- [MT04] F. Mazzia and D. Trigiante. A hybrid mesh selection strategy based on conditioning for boundary value ODE problems. *Numerical Algorithms*, 36(2):169–187, 2004.
- [NPS11] I. Neitzel, U. Prüfert, and Th. Slawig. A smooth regularization of the projection formula for constrained parabolic optimal control problems. *Numer. Funct. Anal. Optim.*, 32(12):1283–1315, 2011.
- [Pam01] Th. Pampel. Numerical approximation of connecting orbits with asymptotic rate. *Numerische Mathematik*, 90(2):309–348, 2001.
- [RZ99a] J. P. Raymond and H. Zidani. Hamiltonian Pontryagin’s principles for control problems governed by semilinear parabolic equations. *Appl. Math. Optim.*, 39(2):143–177, 1999.

- [RZ99b] J. P. Raymond and H. Zidani. Pontryagin's principle for time-optimal problems. *J. Optim. Theory Appl.*, 101(2):375–402, 1999.
- [SBB<sup>+</sup>09] M. Scheffer, J. Bascompte, W. A. Brock, V. Brovkin, St. R. Carpenter, V. Dakos, H. Held, E. H. van Nes, M. Rietkerk, and G. Sugihara. Early-warning signals for critical transitions. *Nature*, 461:53–59, 2009.
- [Ski78] A. K. Skiba. Optimal growth with a convex-concave production function. *Econometrica*, 46(3):527–539, 1978.
- [Trö10] Fredi Tröltzsch. *Optimal control of partial differential equations*, volume 112 of *Graduate Studies in Mathematics*. American Mathematical Society, Providence, RI, 2010.
- [Uec15] H. Uecker. Optimal control and spatial patterns in a semi arid grazing system. Preprint, 2015.
- [UWR14] H. Uecker, D. Wetzel, and J. Rademacher. pde2path – a Matlab package for continuation and bifurcation in 2D elliptic systems. *NMTMA*, 7:58–106, 2014. see also [www.staff.uni-oldenburg.de/hannes.uecker/pde2path](http://www.staff.uni-oldenburg.de/hannes.uecker/pde2path).